THE ASTROPHYSICAL JOURNAL, 582:919–923, 2003 January 10


# A SCATTERED LIGHT ECHO AROUND SN 1993J IN M81

JI-FENG LIU, JOEL N. BREGMAN, AND PATRICK SEITZER
Department of Astronomy, University of Michigan, Ann Arbor, MI 48109
*Received 2002 June 4; accepted 2002 September 16*

## ABSTRACT

A light echo around SN 1993J was observed 8.2 yr after explosion by a *Hubble Space Telescope* Wide Field Planetary Camera 2 observation, adding to the small family of supernovae with light echoes. The light echo was formed by supernova light scattered from a dust sheet that lies 220 pc away from the supernova, 50 pc thick along the line of sight, as inferred from the radius and width of the light echo. The dust inferred from the light echo surface brightness is 1000 times denser than the intercloud dust. The graphite-to-silicate fraction cannot be determined by our *BVI* photometric measurements. However, a pure graphite model can be excluded on the basis of comparison with the data. With future observations, it will be possible to measure the expansion rate of the light echo, from which an independent distance to M81 can be obtained.

*Subject headings:* dust, extinction — galaxies: individual (M81) — scattering — supernovae: individual (SN 1993J)

## 1. INTRODUCTION

Shortly after the burst of Nova Persei 1901, a light echo was observed to emerge with superluminal expansion. It was later properly explained (Couderc 1939) to be the nova light scattered by dust nearby that reached us later than the unscattered photons because of light travel effects. The possibility of observing such an effect with supernovae was later discussed by many authors (e.g., Schaefer 1987). More than its splendid appearance, a light echo also sheds light on the circumstellar and interstellar environments through which it passes, the most famous example being SN 1987A in the Large Magellanic Cloud. Observations of reemission from the rings around SN 1987A provide us with information on the geometry, distribution, and composition of its circumstellar medium (e.g., Lundqvist & Fransson 1991), help us to infer the stellar wind history of its progenitor, and even enable us to determine an accurate distance to SN 1987A (Panagia et al. 1991). Also, the monitoring of its scattered light echoes enables a three-dimensional mapping of the structure of the interstellar medium in front of SN 1987A (Xu, Crotts, & Kunkel 1995), which reveals aspects of dense clouds and superbubbles that are difficult to reveal by other means.

One important application of a light echo is its potential in determining the distance of the supernova and its host galaxy by associating the observed angular scales with corresponding physical scales in the vicinity of the supernova. One example is the elliptical ring around SN 1987A, whose physical size can be determined by studying the light curves of emission lines from the ring excited by illumination of the supernova flash. By comparing the physical size and angular size of the ring, the distance to SN 1987A was determined rather accurately (e.g., $51.2 \pm 3.1$ kpc: Panagia et al. 1991; $46.77 \pm 0.76$ kpc: Gould 1995). Sparks (1994) suggested determining the distances using polarized light echoes, based on the idea that polarization from electron scattering maximizes at a scattering angle of 90°. The polarized light echo expands at the speed of light ($c$), and the distance ($D$) can be obtained by the relation $D = ct/\theta$ ($\theta$ is the observed angular size at time $t$ after supernova explosion). Another way is to make consecutive observations to obtain the expansion rate of the (scattered) light echo. When compared to model calculations that invoke the physical scales in the vicinity of the supernova, these observations can be used to calculate the distance to the supernova. Recently, Munari et al. (2002) reported the emerging of a light echo around V838 Mon after the nova erupted in 2002 January. Munari et al. (2002) estimated a distance of 790 pc by assuming a spherical expansion of the echo.

Light echoes of supernovae have also been found in distant galaxies. For example, SN 1991T, a luminous Type Ia supernova in NGC 4527, exhibited a nearly flat light curve more than 950 days after maximum light and spectral features that, although present in earlier spectra, were substantially narrower and blueshifted on a significantly bluer continuum (Schmidt et al. 1994). Schmidt et al. (1994) attributed these features to a light echo, which was later confirmed by *Hubble Space Telescope* (*HST*) Faint Object Camera observations (Sparks et al. 1999). Similar photometric and spectroscopic behaviors in the late-time observations of SN 1998bu have led to the suggestion of a light echo (Cappellaro et al. 2001), but it has yet to be confirmed by direct high-resolution imaging.

On account of limited spatial resolution, direct imaging observations of supernova light echoes are possible only in our local supercluster, which makes these phenomena rare events. Thus far, only Nova Persei 1901, Nova V838 Mon, SN 1987A, SN 1991T, and SN 1998bu are reported to have associated light echoes in the literature. Here we report on a light echo around SN 1993J, which we use to estimate the grain properties in front of SN 1993J.

The supernova SN 1993J exploded on 1993 March 28 in the spiral galaxy M81, and owing to its proximity (3.6 Mpc), it has been observed at wave bands from radio to $\gamma$-rays. It began as a Type II supernova, but changed later to Type Ib at the nebular stage and was classified as Type IIb. A series of observations with the Very Large Baseline Interferometer revealed an expanding radio shell that was decelerating (Bartel et al. 2000), reflecting the interaction between the shock front and the circumstellar medium. Intensive photometric and spectroscopic observations also showed an infrared excess after day 50 that may be indicative of an infrared echo (Lewis et al. 1994).

In this paper we report an optical scattered light echo around SN 1993J that was discovered in an *HST* Wide Field Planetary Camera 2 (WFPC2) observation. In § 2 we discuss our observations showing the light echo and another archive *HST* WFPC2 observation with a nondetection of such a light echo. In § 3 models for this light echo are discussed, which give the geometry and dust properties. For the distance to SN 1993J, we use the distance to M81, i.e., 3.63 Mpc ($\mu = 27.8 \pm 0.2$: Freedman et al. 1994).

## 2. OBSERVATIONS

As part of an observation of a different target, the WFPC2 was oriented so that SN 1993J fell on a Wide Field chip (WF4) during our 2000 s *HST* observations in the *B*, *V*, and *I* bands (F450W, F555W, and F814W). The observation was obtained on 2001 June 4, 8.2 yr after its explosion; the data were analyzed following standard procedures. In Figure 1 we show four $10'' \times 10''$ images centered on SN 1993J as observed in 1995 and 2001. While SN 1993J appears to be extended, it is consistent with being a point source. Its radial profiles can be fitted by a Gaussian with a FWHM of 1.5 pixels for the WF4 images (1.4 pixels for the 1995 PC image). In the 1995 observation, diffraction patterns were present that are sometimes confused with extended emission. A light echo is clearly visible around SN 1993J that is most obvious in the F555W image and has a radius of about $1\farcs9$ (19 pixels) and a thickness of about $0\farcs2$, which is twice the FWHM of the Wide Field camera ($\sim 0\farcs1$). This ring is a partial arc with the brightest part being about $4\farcs3$ in length. For comparison, another WFPC2 observation on 1995 January 31 (i.e., 1.8 yr after SN 1993J) with the supernova centered in the Planetary Camera was also extracted from the Multimission Archive at STScI. We found no evidence of similar light echoes or partial arcs in the 1995 observation.

The surface brightness of the brightest section of the arc was computed from the arc pixels that are brightest and uncontaminated in the F555W image. Also excluded were those pixels that showed a faint point source in the F814W image. The background mean and sigma were computed from a square box centered on the arc, but excluding the arc and point sources. The net count rates (in DN s$^{-1}$ pixel$^{-2}$) were then converted to surface brightness (in mag arcsec$^{-2}$) using the zero points appropriate for *BVI* photometry (F450W = 22.018, F555W = 22.573, and F814W = 21.688; Whitmore 1995). The listed magnitudes should be accurate to 10%, since no color or charge transfer inefficiency corrections were applied. The measured surface brightness and lower/upper limits in units of mag arcsec$^{-2}$ for 1 $\sigma$ errors in count rates are listed in Table 1. The mean surface brightness of the entire arc is naturally lower; e.g., Sugerman & Crotts (2002) obtained mean surface brightness about 1 mag greater than those listed in Table 1. For the 1995 observation, the 3 $\sigma$ detection threshold in the F555W image, defined by the standard deviation of the mean of a region that includes the positions of the observed $1\farcs9$ arc and the

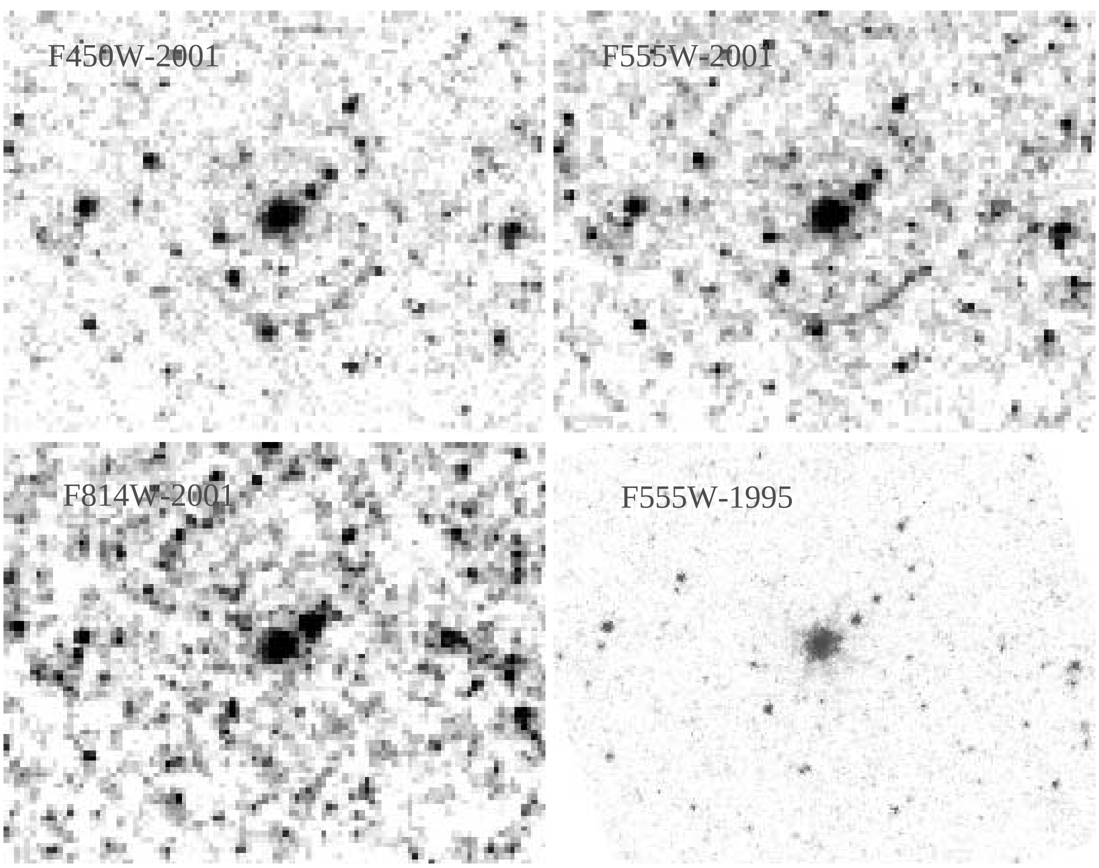


FIG. 1.—Partial arc of a light echo around SN 1993J in the *HST* WFPC2 F450W, F555W, and F814W observations from 2001 June. All images are $10'' \times 10''$ in size. The partial arc is brightest in the F555W and F450W images and has a radius of $1\farcs9$, a width of $0\farcs2$, and an arc length of $4\farcs3$. We do not detect comparable features in an earlier observation (1995 January 31).

TABLE 1

Surface Brightness of the Light Echo

| Filter | Brightness | Lower Limit | Upper Limit |
|---|---|---|---|
| F450W($B$) .............. | 22.6 | 23.8 | 22.5 |
| F555W($V$) ............. | 22.3 | 22.4 | 22.2 |
| F814W($I$) .............. | 22.5 | 22.8 | 22.2 |

postulated 0".9 arc (see § 3), is $\sim$25.2 mag arcsec$^{-2}$, about 15 times fainter than the observed light arc.

Recently, Sugerman & Crotts (2002) have discussed the light echo around SN 1993J, but there is one significant difference from our result: they discuss two extra light arcs, one to the northeast side of the supernova in the 2001 observation, and one to the southwest side of the supernova in the 1995 observation. At the position of their northeast arc, we find a filamentary structure, like other fluctuation structures across the chip. To measure its surface brightness, we excluded point sources from a selected background region and the arc region. The resulting surface brightness corresponds to $6.4 \pm 9.2$ DN pixel$^{-1}$, i.e., below 1 $\sigma$ level. For their southwest arc in the 1995 images, we find no structures at the 3 $\sigma$ level (i.e., $\sim$25.2 mag arcsec$^{-2}$) after excluding the point sources there.

## 3. DISCUSSION

Scattered light seen time $t$ after the supernova onset must be scattered by dust on a $t$ ellipsoid, as illustrated in Figure 2. In the vicinity of the supernova, this ellipsoid can be approximated by a paraboloid. For a dust cloud in front of the supernova, the distance $l$ to the supernova along the line of sight can be obtained for a specified time delay $t$ and

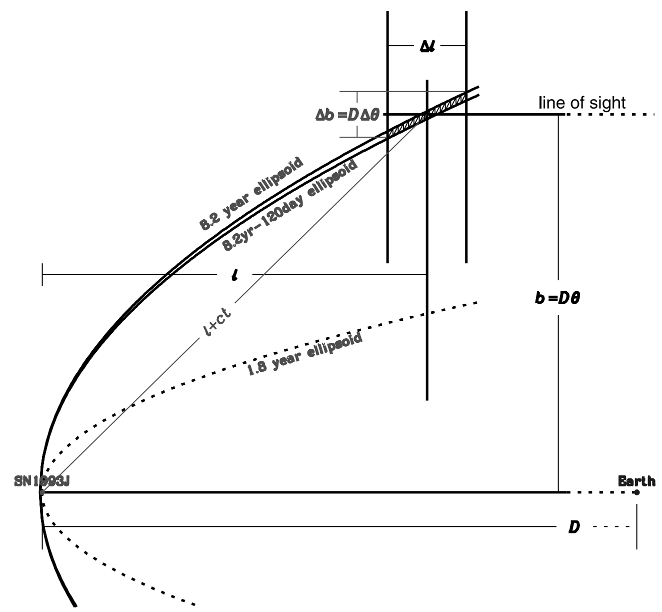


Fig. 2.—Formation of the scattered light arc around the supernova observed 8.2 yr after SN 1993J. The 8.2 yr ellipsoid is the scattering location for light radiated at the supernova explosion, and the 8.2 yr–120 day ellipsoid is for light radiated 120 days after the supernova explosion. The shaded area between the 8.2 yr ellipsoid and 8.2 yr–120 day ellipsoid indicates the dust volume that truly contributes to the scattered light. The symbols are explained in the text.

the impact parameter $b$ (i.e., the perpendicular distance from the supernova to the line of sight, $b = D\theta$, where $D$ is the distance to the supernova from the Earth, and $\theta$ is the angle of the line of sight from the supernova), from the expression $(l + ct)^2 = b^2 + l^2$. For this light echo of SN 1993J, $t = 8.2$ yr, $\theta \approx 1''.9$, or $ct = 2.5$ pc, $b \approx 33.4$ pc, which leads to $l \sim 220$ pc. This distance, as well as the asymmetric shape of the light echo, indicates that the dust cloud could not have originated from the red supergiant wind of the SN 1993J progenitor. Instead, it is most likely a discrete interstellar dust sheet, as seen in our Galaxy. The thickness of the dust sheet along the line of sight can be associated with the width of the light echo by $\Delta l = (b/ct)\Delta b$. The observed values, $\Delta\theta = 0''.2$ or $\Delta b \sim 3.5$ pc, indicate that the dust sheet has a thickness of about 50 pc. The geometry described here is illustrated in Figure 2. Note, however, that the sheet structure in Figure 2 is not the only possible configuration. The detection of this light echo only requires dusty clouds filling the volume between the 8.2 yr ellipsoid and the 8.2 yr–120 day ellipsoid, as shaded in Figure 2.

If this dust sheet extended toward the supernova and crossed the dashed 1.8 yr ellipsoid in Figure 2, a light echo should have been detected in the 1995 WFPC2 observation, with $b \sim 15.8$ pc, or $\theta \approx 0''.9$. The nondetection of such a light echo indicates that either the sheet of gas and dust does not extend closer to the supernova or that it becomes more extended along the line of sight and less dense, which diminishes the surface brightness of the echo. In the 1995 observation, the geometrical path length along the line of sight within the shaded dust volume is longer than in the 2001 observation by a factor of about 4.6. Therefore, for a uniform sheet, the light echo would have been 4.6 times brighter in 1995 than in 2001. Given our upper limit to the light echo for the 1995 observation, we conclude that the dust density of the dust sheet crossing the 1.8 yr ellipsoid should be $15 \times 4.6 \simeq 70$ times less than that in the dust sheet detected by the light arc in the 2001 data. The cloud extension is also limited by the length of the arc, which indicates that the dust sheet is at least 60 pc wide.

The surface brightness of the scattered light arc is, in units of flux per square arcsecond,

$$\Sigma_\lambda(b) = \int_{l_0-\Delta l/2}^{l_0+\Delta l/2} \frac{dl}{\Delta l} F_{\lambda,0} 10^{-0.4 m_\lambda(\tilde{t})} \frac{D^2}{4\pi r^2 \epsilon^2} \times N_d \int_{a_1}^{a_2} f(a) da \pi a^2 Q_{\lambda,\,\mathrm{sca}} F_\lambda(\alpha)\ , \qquad (1)$$

$$2c(t-\tilde{t})l + c^2(t-\tilde{t})^2 - b^2 = 0\ . \qquad (2)$$

In the above equations, $F_{\lambda,0}$ is the flux of magnitude 0, $l_0$ and $\Delta l$ are the location and thickness of the dust sheet, as explained in the above subsection, $\epsilon$ is the factor (=206,265) used to convert arcseconds to radians, $r$ is the distance between the supernova and the scattering point, and $t$ is the time for light echo observations after supernova explosion; $N_d$ is the dust column density in units of grain cm$^{-2}$, $a$ is the radius of the grain, and $f(a)$ is the normalized grain size distribution; $Q_{\lambda,\,\mathrm{sca}}$ is the scattering efficiency of the dust; and $F_\lambda(\alpha)$ is the phase function as in Schaefer (1987), where $\alpha$ is the scattering angle. The quantity $\tilde{t}$ is the elapsed time since the supernova explosion, and $m_\lambda(\tilde{t})$ is the observed light curve (no reddening correction), for which we took the $UBVRI$ photometry of the first 120 days (cf. Lewis et al. 1994). The second equation determines which part of the light curve $m(\tilde{t})$ is scattered by dust at location $l$ on a $t$ ellipsoid.

The existence of interstellar dust has long been established from, for example, the interstellar extinction curve. Fitting to the interstellar extinction curve gives the composition and size distribution when combined with other constraints such as cosmic abundances, gas-to-dust ratios, interstellar physical conditions, and optical properties of the grains. Mathis, Rumpl, & Nordsieck (1977) conclude that the simplest description that fits the observations and the general constraints is of a mixture of uncoated graphite and silicate grains, with a common power-law size distribution $f(a)da \propto a^{-3.5}da$. This description seems to be valid over the entire sky, giving rise to the approximately uniform interstellar extinction law. Local variations from this composition do exist. For example, Bromage & Nandy (1983) show that the extinction curve toward the Small Magellanic Cloud (SMC) does not show the 2200 Å bump that is due to small graphite grains and conclude that the usual graphite contribution is at least a factor of 7 weaker than the "normal" Galactic dust. In our calculation, we considered models with different mixtures of silicate and graphite, with size limits taken as 0.01–0.25 $\mu$m for silicate grains and 0.005–0.25 $\mu$m for graphite grains (Mathis et al. 1977). The grain properties are taken from Draine & Lee (1984).

In comparison, graphite grains have more absorbing power, which is responsible for extinction, while silicate grains have more scattering power, which is responsible for scattered light. The observed surface brightness and the

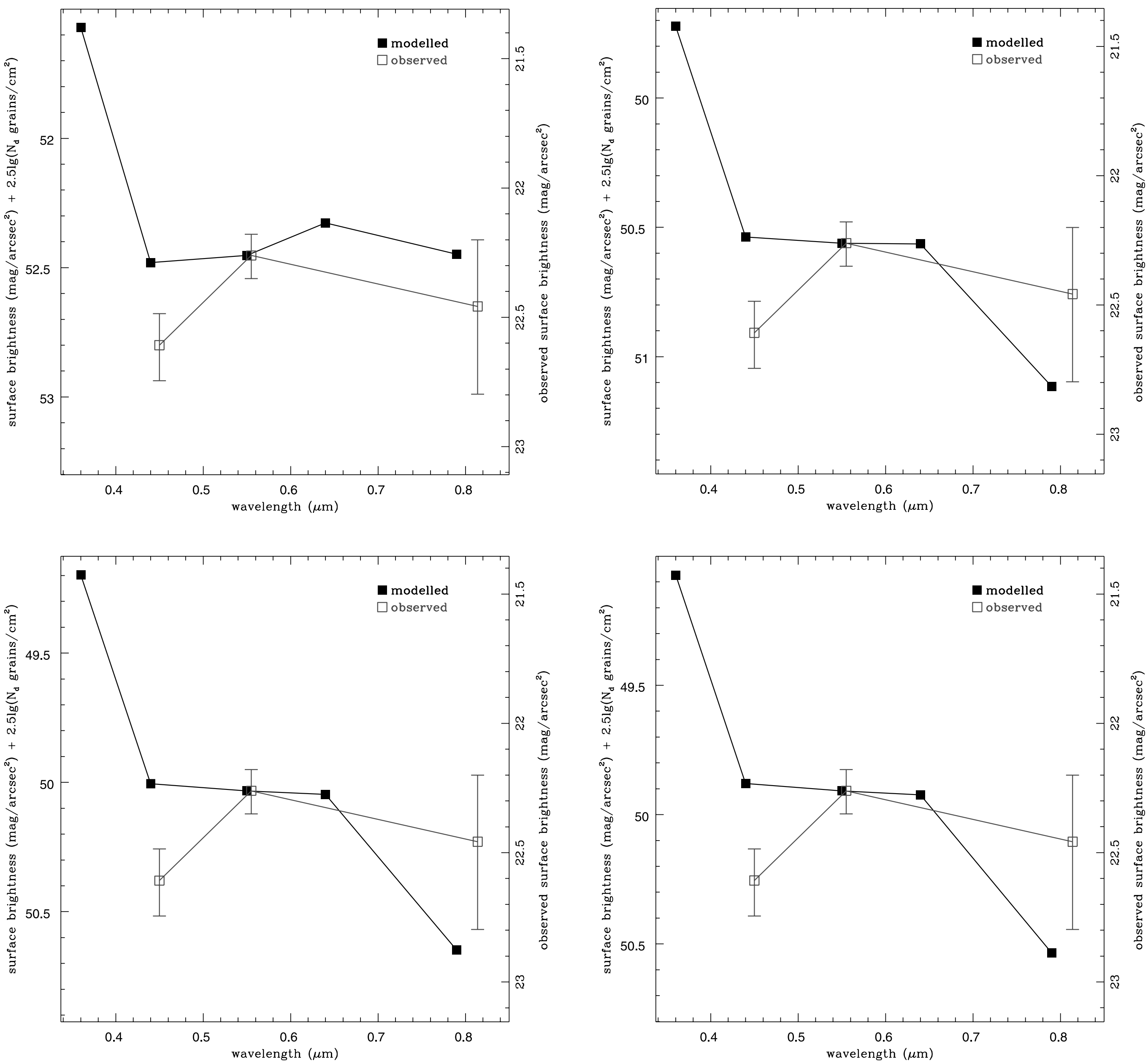


FIG. 3.—Observed and calculated surface brightness of the light echo. The four models, from top to bottom and left to right, are pure graphite model, SMC dust model, normal Galactic dust model, and pure silicate model. The dip in the calculated curve around the $B$ band is due to the fact that the $B$-band light of SN 1993J is much fainter than the redder bands.

calculated values in *UBVRI* for four grain models are shown in Figure 3. By comparing with the observed surface brightness, the grain column density can be obtained. Although the scattering efficiency is greater for blue light, the scattered light in the $B$ band is no brighter than that in the $V$ and $R$ bands, owing to the fact that the supernova light in the $B$ band is much fainter than in redder bands. In our pure graphite model (model A), the scattered light in the $R$ and $I$ bands is much brighter than that in the $B$ and $V$ bands. This feature, however, cannot be used to exclude the pure graphite model due to the large measurement uncertainties. The other models, the Galactic grain model (model B), the SMC grain model (model C), and the pure silicate model (model D), are consistent with the data. For a pure silicate model, comparing measured $V$-band surface brightness with the model, a grain column density of $\sim 1.1 \times 10^{11}$ grains cm$^{-2}$ can be inferred. Given that the dust sheet is about 50 pc wide, this leads to a grain density of $\sim 7.4 \times 10^{-10}$ grains cm$^{-3}$, about 1000 times denser than the intercloud density ($0.5 \times 10^{-12}$ grains cm$^{-3}$; Allen 1976). This density increases when more graphite is introduced into the model. For the Galactic grain model, the inferred grain density is $\sim 1.4 \times 10^{-9}$ grains cm$^{-3}$, which corresponds to a hydrogen column density of $3.9 \times 10^{20}$ cm$^{-2}$ if we adopt an empirical relation of $N_{\rm H} = 5.8 \times 10^{21} E(B-V)$ (Bohlin et al. 1978).

Further constraints may be placed when we consider the extinction of starlight from this dust, which can be obtained by

$$A_\lambda = 1.086 N_d \int_{a_1}^{a_2} \pi a^2 Q_{\lambda,\,\rm abs}(a) f(a) da \,. \quad (3)$$

The extinctions in standard *UBVRI* bands are listed in Table 2 for the four models. The pure graphite model can be rejected by this extinction argument, since a grain column density of $1.2 \times 10^{12}$ grains cm$^{-2}$ is needed to produce the observed surface brightness and will cause an extinction $A_V \sim 1.6$ mag, which is much larger than the observed extinction of SN 1993J of $A_V \sim 0.25$ mag (Richmond et al. 1994) and would have blocked all background stars in the 1995 observation.

TABLE 2

EXTINCTION (mag) FOR FOUR GRAIN MODELS

| Model | $A_U$ | $A_B$ | $A_V$ | $A_R$ | $A_I$ |
|---|---|---|---|---|---|
| A ............. | 2.54 | 2.12 | 1.68 | 1.43 | 1.12 |
| B ............. | 0.37 | 0.30 | 0.23 | 0.20 | 0.15 |
| C ............. | 0.19 | 0.15 | 0.11 | 0.09 | 0.07 |
| D ............. | 0.16 | 0.13 | 0.09 | 0.08 | 0.06 |

## 4. CONCLUSIONS

We have presented the WFPC2 observation of a light echo around SN 1993J 8.2 yr after the supernova explosion. Recently, Sugerman & Crotts (2002) have discussed two extra light echoes that we think are at best marginal detections. The bright light echo is from the supernova light scattered from a dust cloud about 220 pc in front of SN 1993J, about 50 pc thick and 60 pc wide, revealing the existence of a sheet of dust (and gas) in another galaxy. The dust inferred from the light echo surface brightness is 1000 times denser than the intercloud dust. The graphite-to-silicate fraction cannot be determined by our *BVI* photometric measurements. However, a pure graphite model can be excluded based on comparison with the data.

Aside from studying the geometric structure of the interstellar medium in other galaxies, a light echo can be used to determine the distance to the host galaxy. To accomplish this, one needs to measure the expansion rate of the light echo. With future observations, it will be possible to determine this expansion rate and obtain a measurement of the distance independent of that obtained by using Cepheid variables.

We are grateful for the service of the Multimission Archive at STScI (MAST). J. L. thanks Louis-Gregory Strolger and Zheng Zheng for helpful discussions. We gratefully acknowledge support for this work from NASA, grant *HST* GO-09073.01.

## REFERENCES

Allen, C. W. 1976, Astrophysical Quantities (3d ed.; London: Athlone), 265
Bartel, N., et al. 2000, Science, 287, 112
Bohlin, R., Savage, B. D., & Drake, J. F. 1978, ApJ, 224, 132
Bromage, G. E., & Nandy, K. 1983, MNRAS, 204, 29P
Cappellaro, E., et al. 2001, ApJ, 549, L215
Couderc, P. 1939, Ann. d'Astrophys., 2, 271
Draine, B. T., & Lee, H. M. 1984, ApJ, 285, 89
Freedman, W. L., et al. 1994, ApJ, 427, 628
Gould, A. 1995, ApJ, 452, 189
Lewis, J. R., et al. 1994, MNRAS, 266, L27
Lundqvist, P., & Fransson, C. 1991, ApJ, 380, 575
Mathis, J., Rumpl, W., & Nordsieck, K. 1977, ApJ, 217, 425
Munari, U., et al. 2002, A&A, 389, L51
Panagia, N., Gilmozzi, R., Macchetto, F., Adorf, H.-M., & Kirshner, R. P. 1991, ApJ, 380, L23
Richmond, M. W., Treffers, R. R., Filippenko, A. V., Paik, Y., Leibundgut, B., Schulman, E., & Cox, C. V. 1994, AJ, 107, 1022
Schaefer, B. 1987, ApJ, 323, L47
Schmidt, B. P., Kirshner, R. P., Leibundgut, B., Wells, L. A., Porter, A. C., Ruiz-Lapuente, P., Challis, P., & Filippenko, A. V. 1994, ApJ, 434, L19
Sparks, W. B. 1994, ApJ, 433, 19
Sparks, W. B., Macchetto, F., Panagia, N., Boffi, F. R., Branch, D., Hazen, M. L., & della Valle, M. 1999, ApJ, 523, 585
Sugerman, B. E. K., & Crotts, A. P. 2002, ApJ, submitted (astro-ph/0207497)
Whitmore, B. 1995, in Calibrating Hubble Space Telescope: Post Servicing Mission, ed. A. Koratkar & C. Leitherer (Baltimore: STScI), 269
Xu, J., Crotts, A., & Kunkel, W. 1995, ApJ, 451, 806